IOP PUBLISHING JOURNAL OF PHYSICS: CONDENSED MATTER

J. Phys.: Condens. Matter **19** (2007) 406215 (14pp) doi:10.1088/0953-8984/19/40/406215

Effect of particle shape on the density and microstructure of random packings

Alan Wouterse[1], **Stephen R Williams**[2] **and Albert P Philipse**[1]

[1] Van't Hoff Laboratory for Physical and Colloid Chemistry, Debye Institute, Utrecht University, Padualaan 8, 3584 CH, Utrecht, The Netherlands
[2] Research School of Chemistry, Australian National University, Canberra ACT 0200, Australia

E-mail: swilliams@rsc.anu.edu.au and a.p.philipse@chem.uu.nl

Received 23 April 2007, in final form 20 July 2007
Published 12 September 2007
Online at stacks.iop.org/JPhysCM/19/406215

Abstract

We study the random packing of non-spherical particles by computer simulation to investigate the effect of particle shape and aspect ratio on packing density and microstructure. Packings of cut spheres (a spherical segment which is symmetric about the centre of the sphere) are simulated to assess the influence of a planar face on packing properties. It turns out that cut spheres, in common with spherocylinders and spheroids, pack more efficiently as the particle's aspect ratio is perturbed slightly from unity (the aspect ratio of a sphere) to reach a maximum density at an aspect ratio of approximately 1.25. Upon increasing the aspect ratio further the cut spheres pack less efficiently, until approximately an aspect ratio of 2, where the particles are found to form a columnar phase. The amount of ordering is sensitive to simulation parameters and for very thin disks the formation of long columns becomes frustrated, resulting in a nematic phase, in marked contrast to the behavior of long thin rods which always randomly pack into entangled isotropic networks. With respect to coordination numbers it appears that cut spheres always pack with significantly fewer contacts than required for isostatic packing.

(Some figures in this article are in colour only in the electronic version)

1. Introduction

Random particle packings [1] have been widely investigated and form important materials such as granular media (sand, powders), randomly oriented clay particles [2] and fibers in biological cells [3]. Packed particles very often have a non-spherical shape [4–6], which for example is important for shape-induced frustration of hexagonal order in polyhedral colloids [7], random packings of ellipsoids [8] and liquid crystals [9]. Random packings of spheres and spherocylinders further demonstrate the effect of shape on packing properties. Previously we

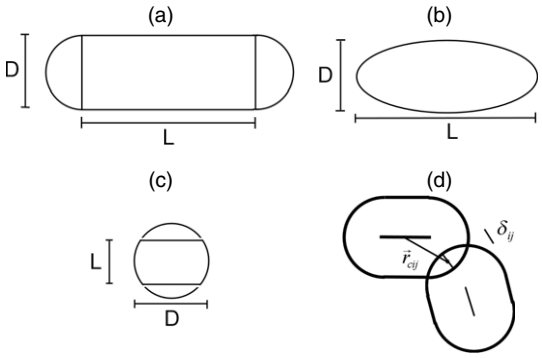

Figure 1. (a) Sketch of a spherocylinder, (b) spheroid and (c) cut sphere with aspect ratios of $(L + D)/D$, L/D and D/L. (d) Graphical illustration of variables that are calculated within the mechanical contraction method: $\vec{r}_{cij}$ connects the contact point to the center of particle i and the distance δ_{ij} quantifies the amount of overlap.

found, using the mechanical contraction method [5], that spherocylinders reach a maximum packing volume fraction upon slightly deviating from a spherical shape. Later Donev *et al* [10] showed, using event-driven molecular dynamics, that spheroids display a similar behavior. To compare these two simulation methods [5, 10] in the present study we apply the mechanical contraction method to spheroids. Both spherocylinders and spheroids are smooth convex objects, which raises the question as to what role this property plays in determining the density as well as the microstructure of a random packing. Therefore we have investigated the random packing of non-smooth particles with planar faces, namely cut spheres (figure 1(c)).

The latter have the advantage that one can gradually transform a sphere-like shape to a disk-like shape with truly planar faces in a controlled way [11], which allows us to study the influence of a flat surface on the packing geometry. The aspect ratio of a cut sphere is defined as D/L, where D is the sphere diameter and L is the thickness. Furthermore, in the limit of large aspect ratio thin cut spheres become identical to short cylinders.

The primary aim of this work is to assess whether characteristic features such as the near-sphere density maximum for spheroids and spherocylinders, which are similar in shape, are particular to these smooth convex bodies or whether this maximum also occurs for particles with planar faces. In addition to the effect of shape on packing density we also investigate the packing microstructure, in particular with respect to the influence of planar faces on orientational correlations.

2. Method

The mechanical contraction method [5] is an attempt to inhibit any overlap between the system's particles by minimally disturbing their positions as the system is compressed. A dilute random configuration of non-overlapping particles is prepared in a cubic box with periodic boundary conditions. In each step of the simulation the volume of the periodic box is reduced by a small amount ΔV and all particle positions are uniformly dilated while their orientations do not change. At a certain number of steps particles start overlapping and this overlap is then removed. The simulation is stopped when it is no longer possible to remove the overlap between particles with a reasonable amount of computational effort. The final configuration is the one from the previous simulation step where none of the particles were overlapping.

To remove overlap between cut spheres or spheroids the overlap removal scheme, as described for the mechanical contraction method for spherocylinders [5], has to be adapted. When two particles i and j overlap, the amount of overlap δ_{ij}, a contact normal n_{ij} and a contact point at the center of the overlap are calculated (figure 1(d)). If particle i is translated and rotated, the rate with which the overlap changes with particle j can be quantified to first order as

$$\frac{\partial \delta_{ij}}{\partial t} = (\vec{v}_i + \vec{\omega}_i \times \vec{r}_{cij}) \cdot \hat{n}_{ij}, \tag{1}$$

where v_i and ω_i are the respective translational and angular velocity and r_{cij} is the vector connecting the contact point with the center of mass of particle i. In order to remove overlap efficiently in the case of C contacts an overlap removal speed s is introduced as

$$s_i = \sum_{j=1}^{C} \delta_{ij} \frac{\partial \delta_{ij}}{\partial t}, \tag{2}$$

where the factor δ_{ij} is included in order to bias the rate at which the particles break contact in favor of those which are overlapping the most. To fix the ratio between translational and rotational velocity a kinetic energy-type constraint is introduced for particle i:

$$\vec{v}_i \cdot \vec{v}_i + \vec{\omega}_i I \vec{\omega}_i = 1, \tag{3}$$

where I is a diagonal matrix that relates to the particle's moment of inertia. The direction which maximizes the rate of overlap removal is sought by the use of Lagrange multipliers with equation (2) and the constraint equation (3) to obtain v_i and ω_i:

$$\vec{v}_i = \sum_{j=1}^{C} \delta_{ij} \hat{n}_{ij} \tag{4}$$

and

$$\begin{aligned}
\omega_i^{(x)} &= \frac{1}{I_{xx}} \sum_{j=1}^{C} \delta_{ij} \left(n_{ij}^{(z)} r_{cij}^{(y)} - n_{ij}^{(y)} r_{cij}^{(z)} \right) \\
\omega_i^{(y)} &= \frac{1}{I_{yy}} \sum_{j=1}^{C} \delta_{ij} \left(n_{ij}^{(x)} r_{cij}^{(z)} - n_{ij}^{(z)} r_{cij}^{(x)} \right) \\
\omega_i^{(z)} &= \frac{1}{I_{zz}} \sum_{j=1}^{C} \delta_{ij} \left(n_{ij}^{(y)} r_{cij}^{(x)} - n_{ij}^{(x)} r_{cij}^{(y)} \right).
\end{aligned} \tag{5}$$

Once v_i and ω_i are calculated, particle i is moved such that it moves half the distance of the smallest δ_{ij}. Particle i is actually displaced slightly further in the simulation to alleviate problems with numerical inaccuracy for small overlaps. The parameter δ_{ov} is an additional displacement that creates a small constant separation between particles. Packings of $N = 4000$ were typically generated with 10^4 attempts to remove overlap between particles and a minimum of $\Delta V = 0.01$. The parameter δ_{ov} was chosen in the range 10^{-2}–10^{-4}. Varying the moment of inertia I_x often leads to slightly denser packings.

2.1. Description of the structure of the generated packings

The following measures were used to describe the structure of the generated packings. Contact numbers were determined by scaling up the cut spheres by a factor s, while keeping the aspect ratio constant, and the resulting overlapping particles were counted as contacts. The number of contacts was then plotted as a function of the threshold, s. A linear extrapolation was employed to obtain the number of contacts when the threshold s is set to zero (figure 2).

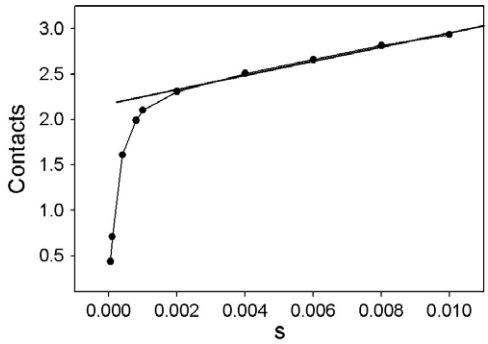

Figure 2. Typical example of the determination of the contact number through a linear extrapolation to zero of the threshold s for cut spheres with aspect ratio 20.

Positional order was measured with the normalized radial pair distribution function (calculated in the same way as for spheres), defined as

$$g(r) = n(r)/(\rho 4\pi r^2 \Delta r) \tag{6}$$

where n is the mean number of cut spheres in a spherical shell Δr at distance r and ρ is the mean number density.

In thermal systems cut spheres can form nematic and columnar phases [11], where in the nematic phase the particles have no positional order but orientational order in one direction; for the columnar phase there is positional order as well as orientational order. To quantify the amount of order in generated packings an orientational alignment matrix Q is used [11], defined as

$$\langle Q \rangle = \frac{1}{N} \sum_{i=1}^{N} \frac{3}{2} \hat{u}_i \hat{u}_i^{\mathrm{T}} - \frac{1}{2} I, \tag{7}$$

where $\hat{u}_i$ is a unit column vector normal to the planar part of a cut sphere, I is the identity matrix and the nematic order parameter is given as

$$S = -2\lambda_0, \tag{8}$$

where λ_0 is the middle eigenvalue of the matrix $\langle Q \rangle$ given by (7). When all vectors u_i point in the same direction then $S = 1$, whereas an isotropic distribution is quantified by $S = 0$.

From the graphical renderings (figure 6) of the packings it was indeed found that the cut spheres tend to align in columns. Whether or not a particle belongs to a column was determined via two threshold values, namely δ_{pc} to decide whether or not the particle's face is nearly parallel with that of its neighbor and δ_{nc} to assess whether or not the particle's centre is close enough to its neighbor in the direction given by the neighbor's axis of symmetry. The criterion for a particle in a column can then be stated as $|\hat{u}_i \cdot \hat{u}_j| > 1 - \delta_{\mathrm{pc}}$ and $|\vec{r}_{ij} \cdot \hat{u}_j| < L + \delta_{\mathrm{nc}}$ together with $|\vec{r}_{ij}| < D$, where $\vec{r}_{ij}$ is a vector connecting the two centers of a pair of cut spheres. The average column length L_{col} is given by $L_{\mathrm{col}} = N_{\mathrm{col}} L$, where L is the thickness of the cut sphere and N_{col} is the average number of particles per column. We note that these criteria are not sensitive to columns, which have been deformed by having particles slide perpendicular to their axis of symmetry, and that this sensitivity becomes more acute as the disks become thinner. While we will not pursue this here we could test for this effect by introducing a third parameter δ_{sc} with the condition, $\frac{1}{2}|\vec{r}_{ij} - \vec{r}_{ij} \cdot \hat{u}_i \hat{u}_i| + \frac{1}{2}|\vec{r}_{ij} - \vec{r}_{ij} \cdot \hat{u}_j \hat{u}_j| < \delta_{\mathrm{sc}}$.

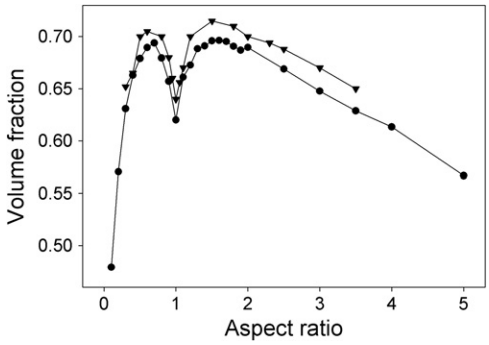

Figure 3. Volume fraction as a function of aspect ratio for spheroid packings. Spheres at aspect ratio one form a singular point. (triangles) Event-driven simulation from Donev *et al* [10], (circles) MCM for spheroids.

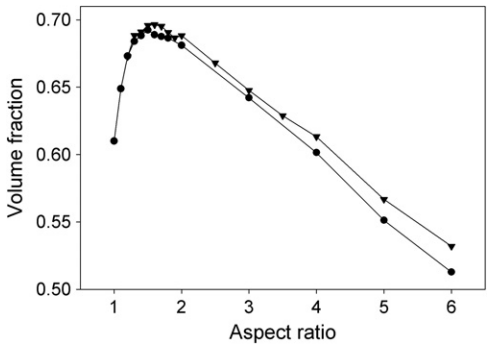

Figure 4. Volume fraction dependence as a function of aspect ratio for spherocylinders (circles) and spheroids (triangles) simulated with the mechanical contraction method.

3. Results and discussions

3.1. Comparison of spherocylinders and spheroids

The volume fractions obtained for oblate and prolate spheroids using the mechanical contraction method (MCM) are plotted in figure 3 and compared to event-driven molecular dynamics simulations of spheroids [10].

As can be seen from figure 3, though event-driven simulation produces slightly higher volume fractions, the dependence of volume fraction on aspect ratio is qualitatively the same for both methods. Using the MCM method a comparison between spherocylinders and spheroids can now be made (figure 4). To compare spherocylinders with spheroids, we do not use L/D (as previously [5]) for the aspect ratio for spherocylinders but $(L + D)/D$ instead (and L/D for spheroids).

Figure 4 shows that spheroids and spherocylinders exhibit a very similar dependence of volume fraction on aspect ratio. It would be interesting to see whether an event-driven molecular dynamics simulation of spherocylinders shows the same behaviour but with a slightly higher volume fraction than was the case for spheroids. Both spheroids and spherocylinders show a maximum in volume fraction at an aspect ratio of roughly 1.5, close to that of spheres,

which in figure 4 have an aspect ratio of 1. Spherocylinders, at least in our simulations, pack slightly less efficiently than spheroids. It is known [5, 6] that for sufficiently high aspect ratios the volume fraction scales inversely proportional to the excluded volume, and if we assume that the average number of contacts to constrain a long spheroid or spherocylinder does not differ much, we can attempt to relate the trend in figure 4 to a difference in excluded volume. The orientationally averaged excluded volume for equal spheroids [12] with volume V_{spheroid} is

$$\frac{V_{\text{ex}}}{8V_{\text{spheroid}}} = \frac{1}{4} + \frac{3}{16}z\left[1 + \frac{(1-\varepsilon^2)}{2\varepsilon}\ln\left(\frac{1+\varepsilon}{1-\varepsilon}\right)\right]\left[\sqrt{1-\varepsilon^2} + \frac{\arcsin(\varepsilon)}{\varepsilon}\right], \tag{9}$$

where $z = L/D$ for prolate spheroids and D/L for oblate spheroids and $\varepsilon^2 = 1 - 1/z^2$, whereas the orientationally averaged excluded volume for spherocylinders [13] is

$$V_{\text{ex}} = (4/3)\pi D^3 + 2\pi L D^2 + (\pi/2)DL^2. \tag{10}$$

In the high-aspect-ratio limit we expect the scaling [6]

$$\phi \sim \langle c\rangle \frac{V_p}{V_{\text{excl}}}; \qquad L/D \gg 1, \tag{11}$$

which for thin spherocylinders becomes

$$\phi \sim \frac{\langle c\rangle}{2}\frac{D}{L}; \qquad L/D \gg 1, \tag{12}$$

whereas for spheroids substitution of equation (9) in (11) yields the asymptote:

$$\phi \sim \frac{4\langle c\rangle}{3\pi}\frac{D}{L}; \qquad L/D \gg 1. \tag{13}$$

This suggests that in the thin-rod limit spherocylinders actually pack slightly more densely than spheroids. Possibly the small difference between spherocylinders and spheroids (which is reproducible) in figure 4 is therefore related to details of the contraction method. Next the effect of a planar face on packing properties is investigated upon cutting equal slices from a sphere.

3.2. Effect of a planar face on packing properties

Cut spheres with a low aspect ratio, i.e. a particle with a small planar face relative to the total surface, show similar packing properties to those for the smooth curved particles discussed previously. A slight deviation from a spherical shape leads to an increase in volume fraction (figure 5(b)). However, upon increasing the contribution of the planar face, we find significantly different packing effects in comparison to smooth convex particles. For large aspect ratios the volume fraction clearly differs from the results for curved particles. The planar face induces considerable alignment and ordering of particles that reduces the excluded volume and, consequently, allows for a denser packing. Such an ordered packing cannot be considered random anymore. At small aspect ratios random packings of cut spheres are insensitive to simulation parameters, and we expect that different techniques, such as molecular dynamics and experiments, should be able to reproduce these results. At high aspect ratios the degree of ordering depend sensitively on the simulation parameters. Such alignment, of course, would also increase the packing density for high-aspect ratio (sphero)cylinders. However, in the latter case the thin rods form entangled structures that prohibit local alignment, which appears to be an essential difference between packings of high-aspect-ratio rods and disks.

When the parameters in the simulation are varied in order to maximize the density, the cut spheres of larger aspect ratio start to crystallize in a columnar phase. This can be seen in figure 5(a), where large fluctuations in the volume fractions obtained from individual

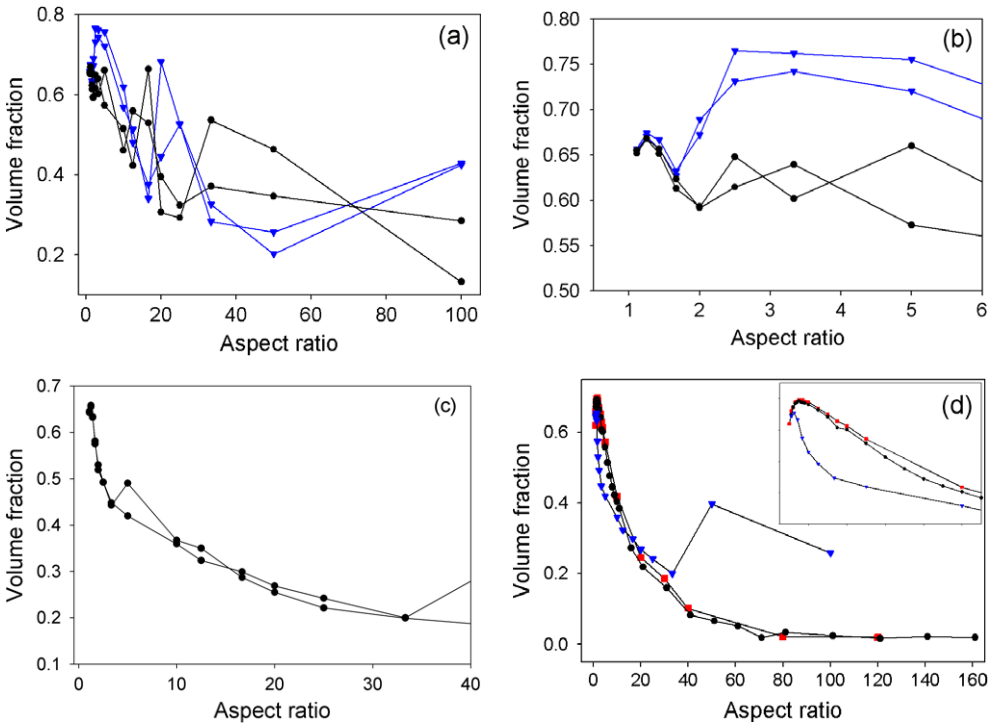

Figure 5. (a) Volume fraction dependence for the packing of cut spheres as a function of aspect ratio. The spikes are caused by a columnar phase of the crystallized packing. Two simulations that only differ in starting configuration are shown for two cases with varying δ_{ov}: (triangles) $\delta_{ov} = 0.01$ and (circles) $\delta_{ov} = 0.001$. (b) A close-up of (a). A slight deviation from an aspect ratio of 1 (sphere) leads to an increase in volume fraction. (c) Two simulations for cut spheres with $\delta_{ov} = 10^{-4}$. (d) Comparison of spheroids (squares), spherocylinders (circles) and cut spheres (triangles).

simulations are indicative of packings that are sensitive to crystallization. Increasing the aforementioned simulation parameter δ_{ov} results in more order in the packing and shows the sensitive dependence of the packing volume fraction on simulation parameters at aspect ratios where crystalline ordering occurs. Graphical images of various packings, most showing significant crystalline order, may be seen in figure 6. The strong ordering seen here is due to the large value of the parameter $\delta_{ov} = 0.01$ that has been used. However, the ordering only occurs for particles of larger aspect ratio than 2, as can be seen in figure 5(b). The contraction method yields reproducible packings, which are not sensitive to arbitrary simulation parameters below an aspect ratio of 2 where the disordered structures appear stable under compression. We argue that this sensitivity of crystallization on arbitrary simulation parameters is not merely an artifact of our simulation method but is relevant to experimental systems as well. For example friction between particles, the employed packing procedures and other experimental details could all be sensitively important to the propensity of the packing to crystallize. An example of this is the finding of sediments of colloidal platelets [2] that pack less densely than is expected for a columnar phase but agrees well with figure 5(c).

For cut spheres, starting from spherical shape, the volume fraction initially increases with aspect ratio. However, for larger aspect ratios the volume fraction does not decrease as rapidly as it does for spherocylinders and spheroids due to ordering of the cut spheres (figure 5(d)).

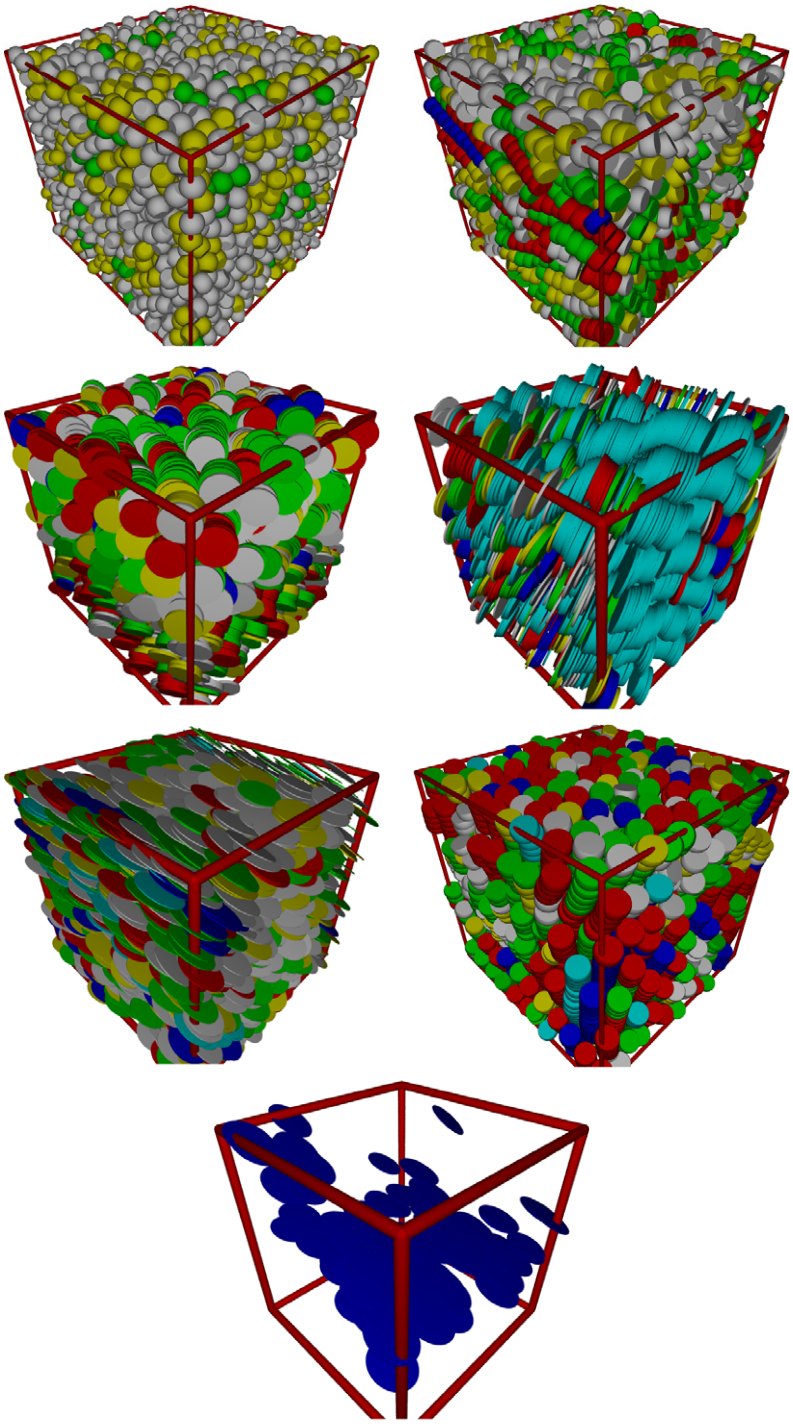

Figure 6. Graphical examples of cut spheres ($N = 4000$) with $\delta_{ov} = 0.01$: (a) aspect ratio 1.25, (b) aspect ratio 2, (c) aspect ratio 10, (d) aspect ratio 20, (e) nematic phase of aspect ratio 50, (f) columnar phase of aspect ratio 2.5, $\varphi = 0.765$. The cut spheres are color coded according to the length of the columns. (g) Illustration of the nematic effect.

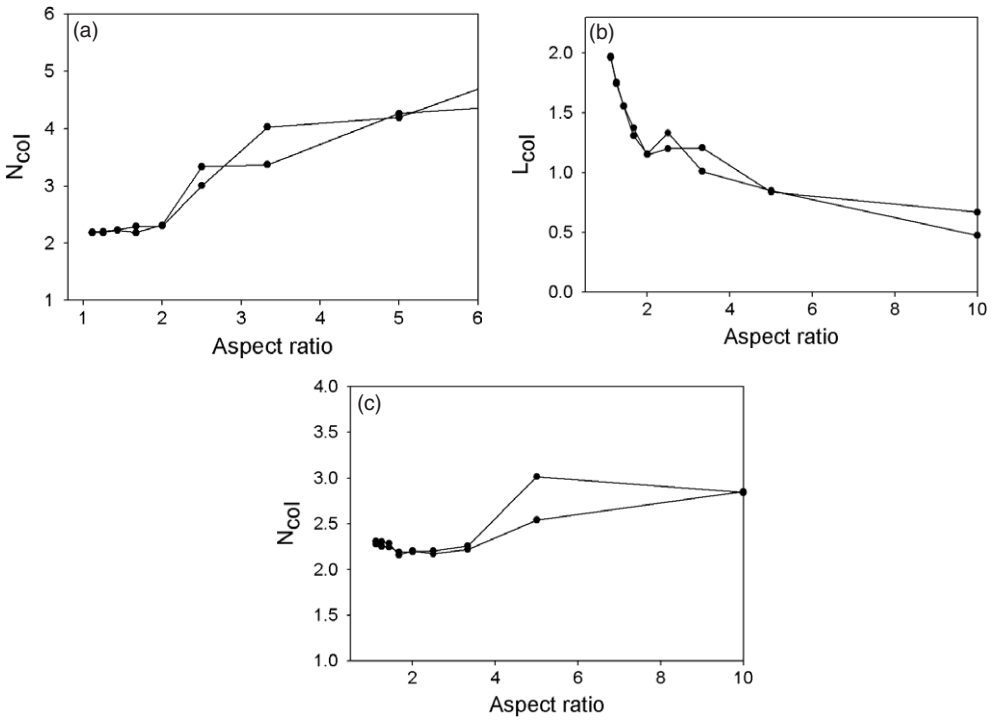

Figure 7. Statistics of columns in cut sphere packings of the two runs, with $\delta_{ov} = 10^{-3}$, that did not exhibit a strong tendency to crystallize. (a) Average number of particles per column $\langle N_{col} \rangle$. (b) Average length of a column $\langle L_{col} \rangle$. (c) Same as (a) but with $\delta_{ov} = 10^{-4}$ which resulted in still less tendency to crystallize.

This can also be seen from the images of cut sphere packings (see figure 6). For spherocylinders and spheroids the excluded volume effects start to dominate for larger aspect ratios where it is not possible to align themselves due to entanglement and jamming, whereas in a cut-sphere packing, the cut spheres can reduce their excluded volume by alignment. The effect of this alignment is that the cut sphere packings mimics a polydisperse packing of cylinders that are formed from a column of connected cut spheres. The volume fraction for polydisperse particle packings is often higher than for monodisperse particle packings [14]. For larger aspect ratios the cylinders that are formed display significant ordering resulting in more efficient packing.

The statistics of the columns seen in figure 6 were studied by computing the average number of cut spheres in a column N_{col} and the average length of a column L_{col} as detailed in section 2, with results shown in figure 7. For large aspect ratios a nematic phase is observed. In this case particles in a stairway-like alignment are being counted as belonging to a single column. An example of this stairway alignment is given in figure 6(g), which is a rendering of only the dark blue particles of figure 6(e) which shows strong orientational but poor positional order, i.e. a nematic phase. Given that the nematic phase can be clearly seen in figure 6 we decided to allow the identification of these stairway like columns rather than use the additional criteria with the parameter δ_{sc} to remove them as discussed in section 2.

The number of particles per column N_{col} increases with aspect ratio (figure 7(a)) but more slowly than the inverse aspect ratio D/L, with the net result that the average column length L_{col} decreases (figure 7(b)).

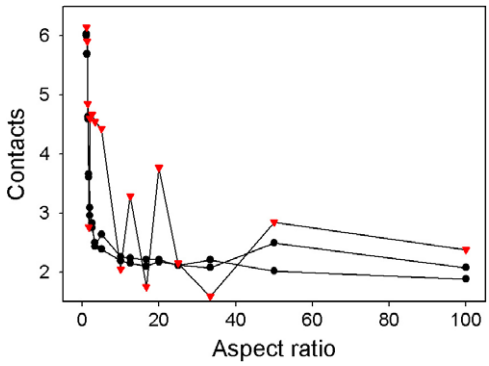

Figure 8. Contact number as a function of aspect ratio for cut sphere packings generated with $\delta_{ov} = 10^{-4}$ (circles) and $\delta_{ov} = 0.01$ (triangles).

3.3. Contact numbers

In a system of particles, ignoring finite size effects, there are Nd degrees of freedom where N is the number of particles and d is the number of degrees of freedom per particle. For a sphere, which has orientational symmetry, we need only consider the translational degrees of freedom and thus $d = 3$. For a cut sphere there is only one, of a possible 3, orientational axis of symmetry and thus $d = 5$. The isostatic conjecture [15] states that the number of constraint equations is at least equal to the number of degrees of freedom Nd and that disordered packings have the minimal number of contacts necessary for mechanical stability. Each contact is shared by two particles and thus, by this conjecture, the average number of contacts per particle, $\langle C \rangle$, is given by $\langle C \rangle = 2d$. Chaikin *et al* [16] provide a convincing argument as to why the isostatic conjecture may fail for non-spherical particles. In particular when the flat faces of a pair of cut spheres are in contact a translational degree of freedom is constrained as well as two orientational degrees of freedom. A pair of cut spheres can constrain three degrees of freedom with a single contact and thus, in this case, one would expect the isostatic conjecture to fail.

The contact number as a function of aspect ratio is shown in figure 8 for the cases $\delta_{ov} = 0.01$ and 10^{-4}. The spikes in the graph for $\delta_{ov} = 0.01$ are indicative of the sensitivity to crystallization. For aspect ratios close to unity the contact number is close to $\langle C \rangle = 6$, which is consistent with the isostatic conjecture for spheres as is well known from previous studies [15, 16]. Consistent with previous work on spherocylinders [5] and spheroids [10] we do not find any evidence for the average contact number rising discontinuously to $\langle C \rangle = 10$ upon departing from spherical symmetry. In [17] it was found that randomly packing the maximum number of spheres does not produce optimal packings and that denser packings are formed by having a contact number lower than the packing number of 8.4. Slightly deforming spheres does not change the volume and surface area dramatically and therefore it is expected that $\langle C \rangle$ will not rise discontinuously to 10 to produce optimal packings for near-spheres. However, in experimental spherocylinder packings the contact number clearly does approach $\langle C \rangle = 10$ at large aspect ratios [18], while experimental data at high aspect ratios have yet to be reported for spheroids. In view of the argument of Chaikin *et al* [16] it is not surprising that we see no evidence of $\langle C \rangle = 10$ for cut spheres, violating the isostatic conjecture due to a single contact being able to constrain more than one degree of freedom.

For high aspect ratios the contact number approaches the limit of approximately 2 for both the disordered and ordered packings, which implies an aligned cut sphere above and below each particle on average. This suggests that almost all the particles in these configurations are

still able to move in the direction of the planar face of the cut sphere (i.e. essentially all the particles are rattlers) and the system is not jammed. In the case of the disordered packings we expect structural integrity to be lacking. While it may be able to support a compressive load under some conditions, it will be very unstable to further ordering.

Again we note the considerable order that the system requires to become tightly packed at large aspect ratios and the apparent frustration in the ordering process. This suggests that the columns may be jammed while the particles forming them are able to slide or rattle in a direction perpendicular to the column. For the crystalline phases, be they columnar or nematic, we argue that structural integrity may be present. The number of contacts, two, is consistent with constraining the particles in a column with the degrees of freedom perpendicular to the column still being free. In the limit of long columns, formed from many cut spheres, and treating each column to be effectively a single particle, we obtain a stable structure. The same can be said for a nematic phase consisting of planes made from very thin cut spheres in the limit of large surface area. In either case the contacts necessary to constrain the columns or planes become insignificant in the limit. Thus we obtain a structure consisting of jammed columns or planes, which are formed from thin disks that are able to slide or rattle in a direction perpendicular to the column or in the plane, respectively.

Two contacts per particle is also consistent with the nematic phase as seen in figure 6(e). There are large fluctuations in the number of contacts when $\delta_{ov} = 0.01$ due to the frustrated ordering process.

3.4. Radial distribution functions

The normalized radial distribution function (rdf) of a random packing of cut spheres with aspect ratio 1.11 is similar to the rdf of a random sphere packing (figure 9(b)) in both computer simulations [17] and experiments [19]. In figure 9(b) there is a small peak at $r = 0.9$ which corresponds to two touching parallel cut spheres (since the thickness of the cut sphere is 0.9) and a peak at $r = 0.95$, due to the contact between a spherical face of one particle with the cut face of another. The columnar crystal phase in figure 9(c) shows considerable structure in the radial distribution function due to the high degree of order present.

The order parameter S as a function of aspect ratio (figure 10) shows interesting behavior. For aspect ratios less than 2.0 the packings are disordered. When the overlap parameter is large, $\delta_{ov} = 0.01$, the influence of the planar face shows up as an increased amount of order with increasing aspect ratio. When the overlap parameter is small, $\delta_{ov} = 10^{-4}$, the system's ability to form an ordered structure is highly frustrated. At aspect ratio 10 the order is lower than expected for an ordered system (figure 10(b)). In these cases the MCM is no longer able to successfully rearrange the system to make it crystallize. Whether or not a system is able to form an ordered structure in an experiment, and if it does at what aspect ratio, very likely also depends on factors such as friction between the particles and the method used to prepare the packing. Nevertheless thin colloidal Gibbsite platelets with an aspect ratio of about 13 were found [2] to pack into a sediment with a volume fraction of around 0.4, which actually agrees quite well with our simulation results in figure 5(c).

4. Conclusions

For the case of spheroids our mechanical contraction method (MCM) produces random packings with a marginally lower volume fraction than existing data generated with event-driven molecular dynamics methods [10]. We have shown in addition that spherocylinders and spheroids exhibit very similar packing behavior, consistent with their similarity in shape,

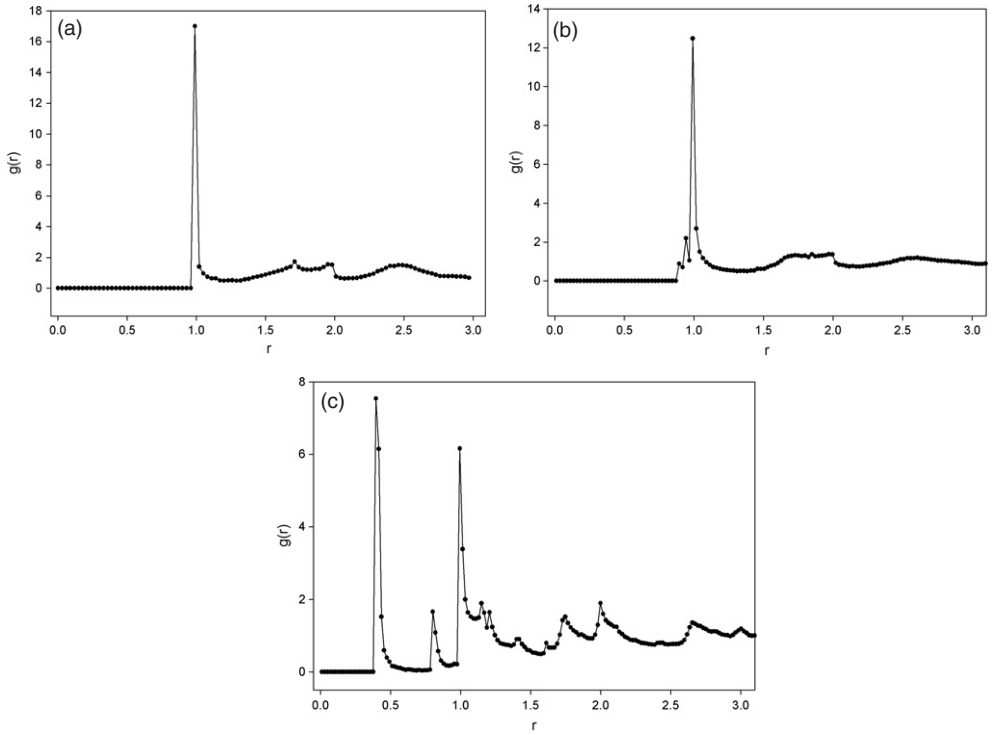

Figure 9. Normalized radial distribution functions: (a) disordered sphere packing, $\delta_{ov} = 10^{-6}$; (b) cut spheres with aspect ratio 1.11 and $\delta_{ov} = 10^{-4}$; (c) columnar crystal of cut spheres with aspect ratio 2.5 and $\delta_{ov} = 0.01$.

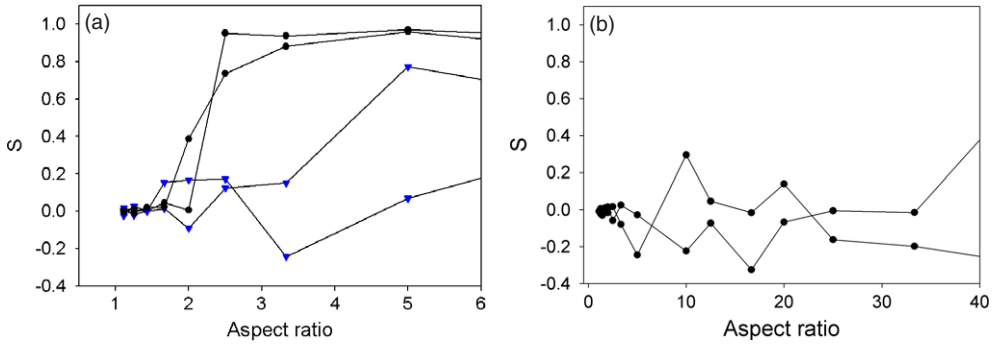

Figure 10. Nematic order parameter S as a function of aspect ratio of cut spheres for simulation runs with parameters (a) $\delta_{ov} = 0.01$ (circles) and 0.001 (triangles) and (b) $\delta_{ov} = 10^{-4}$. Simulations were repeated twice in each instance to check reproducibility.

with respect to the density maximum for near-spheres and the density decrease at higher aspect ratios.

A slight deviation from spheres by the use of cut spheres yields random packings with a higher volume fraction similar to elongating spheres, as with spherocylinders, or deforming spheres, as is the case with spheroids. The low-aspect-ratio (near spherical) cut spheres form disordered packings with similar structure to disordered sphere packings, as shown

by the normalized radial distribution functions. The results for low-aspect-ratio cut spheres are insensitive to simulation parameters and should be reproducible with different simulation techniques. For higher aspect ratios the packing behavior of cut spheres is very different from spheroids and spherocylinders. Under favorable simulation parameters the planar part of the cut sphere promotes order in the packing by particle alignment, which reduces the excluded volume and allows for denser packings than for random packings of high-aspect-ratio spherocylinders and spheroids that form highly entangled structures. Thus, the jamming of thin cut spheres is qualitatively different from jammed packings of spherocylinders and spheroids. Columns of particles are formed with different orientations and the packing can no longer be considered random or disordered. The nematic order parameter increases with aspect ratio, which is indicative of this alignment effect. While at small aspect ratios the obtained disordered packings are not sensitive to simulation parameters, the same cannot be said for the large aspect ratios. Here the tendency to form an ordered structure is sensitive to the chosen simulation parameters and we argue that this is due to the lack of a stable amorphous structure, for thin disks under a compressive load. At these aspect ratios the system is very susceptible to ordering in a manner that depends on the details much more sensitively than is the case for sphere like particles. We conclude that packings of thin disks are far more sensitive to crystallization than is the case for spheres. This is consistent with common intuition, gained from experience with objects such as collections of coins.

The packings generated for the cut spheres are not isostatic, as can be seen from the contact numbers and as expected due to a pair of contacting flat faces constraining more than a single degree of freedom.

Acknowledgments

The Stichting voor Fundamenteel Onderzoek der Materie (FOM), financially supported by the Nederlandse Organisatie voor Wetenschappelijk Onderzoek (NWO), is acknowledged for both general funding and providing support for AW to travel to Australia and stay at the Research School of Chemistry where a significant component of this work took place. We thank the Australian Partnership for Advanced Computing (APAC) for computational facilities.

References

[1] Aste T and Weaire D 2000 *The Pursuit of Perfect Packing* (Bristol: Institute of Physics Publishing)
Cumberland D J and Crawford R J 1987 *The Packing of Particles* (Amsterdam: Elsevier)
[2] van der Beek D, Petukhov A V, Oversteegen S M, Vroege G J and Lekkerkerker H N W 2005 *Eur. Phys. J.* E **16** 253
[3] Miao L, Vanderlinde O, Liu J, Grant R P, Wouterse A, Philipse A P, Stewart M and Roberts T M 2006 to be submitted
[4] Philipse A P, Nechifor A and Patmamanoharan C 1994 *Langmuir* **10** 4451
[5] Williams S R and Philipse A P 2003 *Phys. Rev.* E **67** 051301
[6] Philipse A P 1996 *Langmuir* **12** 1127
[7] Dullens R P A, Mourad M C D, Aarts D G A L, Hoogenboom J P and Kegel W K 2006 *Phys. Rev. Lett.* **96** (2)
[8] Sherwood J D 1997 *J. Phys. A: Math. Gen.* **30** 839
Man W N, Donev A, Stillinger F H, Sullivan M T, Russel W B, Heeger D, Inati S, Torquato S and Chaikin P M 2005 *Phys. Rev. Lett.* **94** (19)
[9] Vroege G J and Lekkerkerker H N W 1992 *Rep. Prog. Phys.* **55** 1241
[10] Donev A, Cisse I, Sachs D, Variano E, Stillinger F H, Connelly R, Torquato S and Chaikin P M 2004 *Science* **303** 990
[11] Veerman J A C and Frenkel D 1992 *Phys. Rev.* A **45** 5632
[12] Isihara A 1951 *J. Chem. Phys.* **19** 1142

[13] Onsager L 1949 *Ann. New York Acad. Sci.* **51** 627
[14] Kristiansen K D, Wouterse A and Philipse A P 2005 *Physica* A **358** 249
Kansal A R, Torquato S and Stillinger F H 2002 *J. Chem. Phys.* **117** 8212
[15] Edwards S F and Grinev D V 1999 *Phys. Rev. Lett.* **82** 5397
[16] Chaikin P M, Donev A, Man W N, Stillinger F H and Torquato S 2006 *Ind. Eng. Chem. Res.* **45** 6960
[17] Wouterse A and Philipse A P 2006 *J. Chem. Phys.* **125** 194709
[18] Blouwolff J and Fraden S 2006 *Europhys. Lett.* **76** 1095
[19] Aste T, Saadatfar M and Senden T J 2005 *Phys. Rev.* E **71** 061302
Aste T 2005 *J. Phys.: Condens. Matter* **17** S2361